



OPEN

Global CO₂ fertilization of *Sphagnum* peat mosses via suppression of photorespiration during the twentieth century

Henrik Serk^{1,2}, Mats B. Nilsson²✉, Elisabet Bohlin², Ina Ehlers¹, Thomas Wieloch¹, Carolina Olid^{2,3}, Samantha Grover⁴, Karsten Kalbitz⁵, Juul Limpens⁶, Tim Moore⁷, Wiebke Münchberger⁸, Julie Talbot⁹, Xianwei Wang¹⁰, Klaus-Holger Knorr⁸, Verónica Pancotto¹¹ & Jürgen Schleucher¹✉

Natural peatlands contribute significantly to global carbon sequestration and storage of biomass, most of which derives from *Sphagnum* peat mosses. Atmospheric CO₂ levels have increased dramatically during the twentieth century, from 280 to > 400 ppm, which has affected plant carbon dynamics. Net carbon assimilation is strongly reduced by photorespiration, a process that depends on the CO₂ to O₂ ratio. Here we investigate the response of the photorespiration to photosynthesis ratio in *Sphagnum* mosses to recent CO₂ increases by comparing deuterium isotopomers of historical and contemporary *Sphagnum* tissues collected from 36 peat cores from five continents. Rising CO₂ levels generally suppressed photorespiration relative to photosynthesis but the magnitude of suppression depended on the current water table depth. By estimating the changes in water table depth, temperature, and precipitation during the twentieth century, we excluded potential effects of these climate parameters on the observed isotopomer responses. Further, we showed that the photorespiration to photosynthesis ratio varied between *Sphagnum* subgenera, indicating differences in their photosynthetic capacity. The global suppression of photorespiration in *Sphagnum* suggests an increased net primary production potential in response to the ongoing rise in atmospheric CO₂, in particular for mire structures with intermediate water table depths.

Over one third of global soil carbon (C) is stored in boreal mires^{1,2}, making peat C accumulation an essential part of the global C budget. Changes in climate are expected to have strong effects on peatland C sequestration^{1,3,4}. During the early and mid-Holocene, the accumulation of peat C was largely determined by the retreat of the northern ice sheet and the rise in temperature because atmospheric CO₂ concentrations were relatively stable at 275 ± 8 ppm (SD)^{5–7}. Since the beginning of the industrial revolution in the early nineteenth century, CO₂ concentrations have risen from ca. 280 ppm to over 400 ppm today⁸. Multiple observations indicate that recent increases in atmospheric CO₂ have affected peat C accumulation rates: (i) the variation in acrotelm peat accumulation was mainly driven by photosynthesis⁹, (ii) peat C accumulation in Alaskan mires increased about threefold during the twentieth century¹⁰, and (iii) the variation in net ecosystem exchange between mires was mainly controlled by differences in leaf area index¹¹. In addition to rising atmospheric CO₂ levels, ongoing climatic changes such as increases in temperature and changes in precipitation are hypothesized to influence peatland C fluxes^{12–14}.

¹Department of Medical Biochemistry and Biophysics, Umeå University, Umeå, Sweden. ²Department of Forest Ecology and Management, Swedish University of Agricultural Sciences, Umeå, Sweden. ³Department of Ecology and Environmental Sciences, Umeå University, Umeå, Sweden. ⁴Department of Applied Chemistry and Environmental Science, RMIT University, Melbourne, Australia. ⁵Institute of Soil Science and Site Ecology, Dresden University of Technology, Tharandt, Germany. ⁶Department of Environmental Sciences, Wageningen University, Wageningen, The Netherlands. ⁷Department of Geography, McGill University, Montreal, Canada. ⁸Institute of Landscape Ecology, University of Münster, Münster, Germany. ⁹Department of Geography, Université de Montréal, Montreal, Canada. ¹⁰Northeast Institute of Geography and Agroecology, Chinese Academy of Sciences, Changchun, People's Republic of China. ¹¹Centro Austral de Investigaciones Científicas (CADIC-CONICET), Ushuaia, Argentina. ✉email: mats.b.nilsson@slu.se; jurgen.schleucher@umu.se

Sphagnum peat mosses are primarily responsible for the accumulation of peat C because they often constitute 80–100% of the ground cover in northern peatlands¹⁵. Compared to vascular plants, *Sphagnum* remnants are highly resistant to microbial decay, which is vital for peat C accumulation^{16,17}. Therefore, C accumulation and storage in the form of *Sphagnum* remains generally exceeds C losses from microbial decay. However, currently it is not clear whether increases in *Sphagnum* C accumulation driven by ongoing and projected global warming will outweigh increases in the rate of microbial peat decomposition^{9,18,19}. Understanding how *Sphagnum* C fluxes respond to recent and projected increases in atmospheric CO₂ is therefore crucial for predicting future peat C fluxes.

To our knowledge, responses of *Sphagnum* photosynthetic C fluxes to the recent increase in atmospheric CO₂ have never been explored on the global scale. Previous attempts to estimate responses of *Sphagnum* to increased atmospheric CO₂ were either based on free-air CO₂ enrichment (FACE) or greenhouse experiments^{20–25}. A recently developed isotopomer method^{26,27} enables reconstruction of metabolic C fluxes by analyzing cell wall carbohydrates from *Sphagnum* remnants. This approach involves using NMR spectroscopy to measure the abundance ratio of the deuterium (D) isotopomers D6^S and D6^R in the C6H₂ groups of glucose derived from hydrolyzed cell wall carbohydrates, where S and R are the stereochemical designators. The abundance ratio of these D isotopomers is correlated with the ratio of Rubisco oxygenation to carboxylation due to D fractionation in the photorespiration pathway²⁶. Therefore, the D6^S/D6^R ratio reflects the relative rates of photorespiration and (gross) photosynthesis which essentially depend on the substrate ratio of CO₂ and O₂. The uptake of C in C₃ plants is facilitated by the carboxylation reaction, catalyzed by the enzyme Rubisco. The oxygenation activity of this enzyme, however, leads to the loss of C and therefore reduces the efficiency of photosynthesis. This process is known as photorespiration, which accounts for C losses of up to 25%, and therefore plays an important role for the global terrestrial C sink²⁸.

Most studies focus on photorespiration in higher plants and only little is known about *Sphagnum* mosses, despite their importance for global peatland C fluxes. Using the isotopomer method, we recently experimentally investigated the response of the photorespiration to photosynthesis ratio (*i.e.* the D6^S/D6^R ratio) to the recent increase in atmospheric CO₂ levels from 280 to 400 ppm and the dependence of this response on selected climate variables including temperature, water table (WT) depth, and light intensity²⁷. We found that under low WT conditions (20 cm below moss surface), photorespiration was suppressed relative to photosynthesis in the hummock species *Sphagnum fuscum*. Under water-saturating conditions (WT near moss surface), however, there was no effect of atmospheric CO₂, indicating that WT depth strongly influences the CO₂ fertilization effect in *S. fuscum*. In addition, the lawn species *S. majus* did not respond to the CO₂ increase, suggesting a species-specific response. Therefore, *Sphagnum* photosynthetic C fluxes are expected to vary with species and microhabitat^{29–32}.

The aim of this study is to investigate changes in *Sphagnum* photosynthetic C fluxes during the twentieth century at the global scale. To do this, we estimated the global response of the photorespiration to photosynthesis ratio by comparing the D6^S/D6^R ratios of modern *Sphagnum* tissues formed at the current atmospheric CO₂ concentration (ca. 400 ppm) to the D6^S/D6^R ratios of *Sphagnum* remnants from peat core sections formed at least 100 years ago under pre-industrial CO₂ concentrations (≤ 300 ppm). Our analysis is based on 36 peat cores from 10 different sites on five continents (Fig. 1A). Effects of microhabitat were tested by including both hummock (n = 25) and lawn (n = 11) samples with WT depths ranging from ≈ 5 to 70 cm below the moss surface. The effect of species was tested by including eight different *Sphagnum* species belonging to three different taxonomic sections (subgenera). To determine whether the CO₂ response of the photorespiration to photosynthesis (D6^S/D6^R) ratio in *Sphagnum* was influenced by changes in temperature and precipitation during the twentieth century, we estimated these changes using established climate models^{33–35}. The effects of changes in WT depth during the twentieth century were estimated using WT reconstruction data available in the literature and by measuring δ¹³C, which has been proposed as proxy for surface moisture^{27,36}.

Results

Global suppression of photorespiration during the twentieth century. Global changes in the photorespiration to photosynthesis ratio during the twentieth century were assessed by comparing the D6^S/D6^R ratios of modern and ≥ 100 years old *Sphagnum* tissues. Modern *Sphagnum* samples were retrieved from surface peat (top 0–2 cm) formed at contemporary atmospheric CO₂ levels (ca. 400 ppm). Conversely, historical *Sphagnum* tissues were retrieved from peat layers ≥ 30 cm below the surface, with an approximate age of 100 years or more (Table S1). Therefore, the historical *Sphagnum* tissues were formed when atmospheric CO₂ concentrations were ≤ 300 ppm. The D6^S/D6^R ratio of modern *Sphagnum* was 0.860 ± 0.004 (average ± SE, range: 0.810–0.927), while that of historical *Sphagnum* was 0.901 ± 0.005 (average ± SE, range: 0.858–0.971, Fig. S1). Thus, the D6^S/D6^R ratio of modern *Sphagnum* was generally lower compared to ≥ 100 years old *Sphagnum*, indicating that photorespiration is suppressed relative to photosynthesis.

The peat samples essentially differed with respect to their depth below the surface (which is related to the atmospheric CO₂ concentration when the *Sphagnum* biomass was formed), the *Sphagnum* subgenus, the present WT depth, and the geographical location (site). The effects of these factors on the D6^S/D6^R ratio were tested by a linear mixed effect model with the site as random factor, and atmospheric CO₂, WT and subgenus as fixed factors. Analysis of variance (ANOVA) of the random factor revealed that the effect of site was not significant (variance = 0.0, *p* = 1.0). ANOVA of the fixed factors showed a significant effect for atmospheric CO₂, WT and subgenus, explaining 35%, 12% and 8% of the variance, respectively (Table 1). A significant interaction was found between CO₂ and WT, which explained 12% of variance, indicating that the effect of CO₂ on the D6^S/D6^R ratio is dependent on the WT depth.

The effect of atmospheric CO₂ on the D6^S/D6^R ratio clearly depended on the present WT depth. The post-hoc test showed that for peat cores where the WT was < 10 cm below the moss surface, the D6^S/D6^R ratios were not

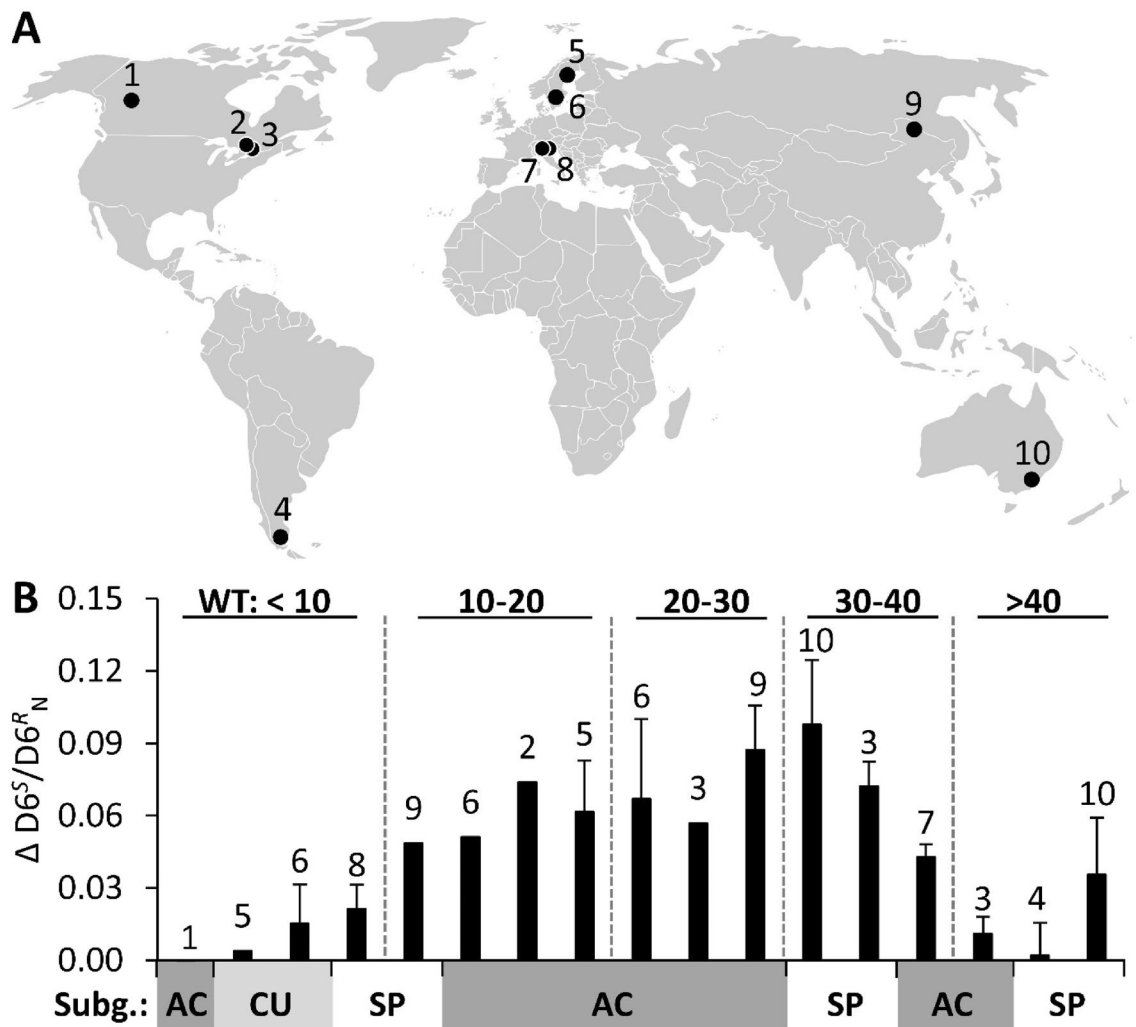


Figure 1. Global changes in the deuterium isotopomer ratio ($\Delta D6^S/D6^R_N$) of *Sphagnum* during the twentieth century representing changes in the photorespiration to photosynthesis ratio. **(A)** Global distribution of investigated sites. **(B)** Response of the $D6^S/D6^R$ ratio per unit change in $1000/[CO_2]$ between modern and historical *Sphagnum* samples ($\Delta D6^S/D6^R_N$). Five water table depths (WT) categories (in cm) are indicated by vertical dashed lines. *Sphagnum* subgenera are indicated on the x-axis by grey/white shading: AC, ACUTIFOLIA (dark grey); CU, CUSPIDATA (light grey); SP, SPHAGNUM (white). Error bars indicate standard error, $n = 1-4$ (see Table S1 for more information). Numbers above error bars correspond to sample sites as numbered in (A).

Factor	Df	F	p	R ²
CO ₂	1, 62	59.75	<0.001	0.35
WT	4, 62	4.87	0.002	0.12
Subg	2, 62	6.36	0.004	0.08
CO ₂ × WT	4, 62	5.05	0.002	0.12
CO ₂ × Subg	n.s.			
WT × Subg	n.s.			
CO ₂ × WT × Subg	n.s.			

Table 1. Summary of ANOVA results for linear mixed effect models of the effects of atmospheric CO₂, water table (WT) and *Sphagnum* subgenus (Subg.) on the $D6^S/D6^R$ ratio. Df, degrees of freedom of the model and residuals. Non-significant factors/interactions with $p > 0.1$ are denoted as n.s.

Site	Δ WT (cm)	Δ MAT ($^{\circ}$ C)	Δ TAP (%)	Reference (WT)
1	≈ 0	+ 3.1	+ 9.9	38
2, 3	+ 4	+ 0.2	- 6.7	39,40
4	- 40*	- 1.7	- 32.6	41
5	$\approx 0^*$	+ 2.8	+ 19.1	37
6	- 5*	+ 1.3	+ 11.1	37,42
7, 8	- 11*	+ 0.4	+ 12.5	37
9	- 6	+ 1.6	+ 25.0	43
10	- 30*	+ 0.1	+ 15.1	44

Table 2. Historical changes in water table depth (Δ WT), mean annual air temperature (Δ MAT) and total annual precipitation (Δ TAP) during the twentieth century at the sites shown in Fig. 1. Changes in TAP are specified in percent change. (-) indicates a decrease and (+) indicates an increase. (*) indicates WT data for another mire in the same region as the relevant site (Table S2).

significantly different ($p > 0.05$, Fig. S1) between modern and historical *Sphagnum*, with means of 0.893 ± 0.01 and 0.905 ± 0.009 (SE), respectively. Conversely, for peat cores with WT depths of 10–40 cm, the $D6^S/D6^R$ ratios of modern and historical *Sphagnum* clearly differed ($p < 0.05$), having means of 0.850 ± 0.004 and 0.910 ± 0.007 (SE), respectively (Figs. 1 and S1). For peat cores with WT depths > 40 cm, the difference between modern and historical samples was again not significant ($p > 0.05$), with means of 0.860 ± 0.007 and 0.873 ± 0.004 (average \pm SE), respectively.

For modern *Sphagnum*, the effect of WT was evident from generally higher $D6^S/D6^R$ ratios for WT depths of < 10 cm (mean 0.893 ± 0.01 SE), compared to samples with WT depths of > 10 cm (mean 0.852 ± 0.007 SE; Fig. S1). For ≥ 100 years-old samples, this was not the case, instead the $D6^S/D6^R$ ratio was generally lower for WT depths > 40 cm (mean 0.873 ± 0.004 SE) compared to WT depths of < 40 cm (mean 0.910 ± 0.01 SE). The *Sphagnum* subgenus also had a clear effect: the mean $D6^S/D6^R$ ratios for modern and historical samples of ACUTIFOLIA species were 0.858 ± 0.004 and 0.906 ± 0.007 (SE), respectively, while those for species of the subgenus SPHAGNUM were 0.846 ± 0.006 and 0.885 ± 0.006 (SE), respectively. The $D6^S/D6^R$ ratio was thus generally lower for species of the subgenus SPHAGNUM than for ACUTIFOLIA species. Modern and historical samples of CUSPIDATA species had higher mean $D6^S/D6^R$ ratios of 0.911 ± 0.008 and 0.921 ± 0.009 (SE), respectively, with no significant difference ($p > 0.05$) between modern and historical samples (Figs. 1 and S1).

The differences in the $D6^S/D6^R$ ratio between modern and historical *Sphagnum* were normalized based on the linear relationship between the $D6^S/D6^R$ ratio and $1000/[CO_2]$ previously reported by Ehlers et al.²⁶, to account for variations in atmospheric CO_2 concentrations due to differences in peat depth and/or age. To this end, the regression slope of this linear function was calculated as the change in the $D6^S/D6^R$ ratio per unit change in $1000/[CO_2]$ between modern and historical *Sphagnum* samples (denoted $\Delta D6^S/D6^R_N$). $\Delta D6^S/D6^R_N$ thus represents the degree of suppression of photorespiration; its mean was 0.044 ± 0.008 (SE) and it varied between 0.000 and 0.094 (Fig. 1). $\Delta D6^S/D6^R_N$ varied with the WT depth: it was 0.010 ± 0.005 (average \pm SE) for WT depths < 10 cm below the moss surface, 0.066 ± 0.006 (average \pm SE) for WT depths between 10 and 40 cm, and 0.016 ± 0.010 (average \pm SE) for WT depths > 40 cm (Fig. 1). These results indicate that a WT between 10 and 40 cm below the moss surface is optimal for suppressing photorespiration in response to increased atmospheric CO_2 .

Effect of changes in water table, temperature and precipitation during the twentieth century. The relationship between $\Delta D6^S/D6^R_N$ and the present WT depth assumes that hydrological conditions were relatively stable over the twentieth century. To test this assumption, we performed a literature review on changes in WT depth during the twentieth century based on previously published testate amoebae WT reconstruction data (Table 2). These literature data were mostly from hummock peat cores with WT depth > 10 cm (except site 1, WT = 8 cm). In cases where data were not available for the sampled mires, data were retrieved for mires from the same region (Tables 2 and S2), assuming that the similarities in regional climate would result in similar changes in WT depth³⁷. Additionally, variations in other climate parameters such as temperature and precipitation may have affected the suppression of photorespiration ($\Delta D6^S/D6^R_N$). Therefore, we also estimated changes in temperature and precipitation during the twentieth century using established climate models^{33–35} (Table 2).

Changes in WT during the twentieth century were generally small (between + 4 and - 11 cm), except in southern Argentina and Australia, where the WT depth decreased by 40 and 30 cm, respectively (Table 2). To determine whether changes in historical climate data contribute to the $\Delta D6^S/D6^R_N$ -response, we performed a three-way ANOVA, with the change in WT (Δ WT), mean annual air temperature (Δ MAT), and total annual precipitation (Δ TAP) as factors. No significant effect of Δ WT, Δ MAT and Δ TAP could be detected ($p > 0.2$). However, a significant interaction was found between Δ WT and Δ MAT ($R^2 = 0.16$, $F = 53.8$, $p = 0.028$). Further, we tested if specifically the changes in mean summer air temperature (Δ MSTAT) or the total summer precipitation (Δ TSP) affect the $\Delta D6^S/D6^R_N$ -response by performing a three-way ANOVA with Δ WT, Δ MSTAT and Δ TSP as factors. Again, no significant effect could be detected ($p > 0.2$), except for an interaction between Δ WT and Δ MSTAT ($R^2 = 0.17$, $F = 53.3$, $p = 0.029$). Thus, a small part of the variation in $\Delta D6^S/D6^R_N$ (17%) of *Sphagnum* may be explained by combined changes in WT and temperature during the twentieth century. Additionally, we performed principal component analysis (PCA) to compare the relationship between the $\Delta D6^S/D6^R_N$ -response

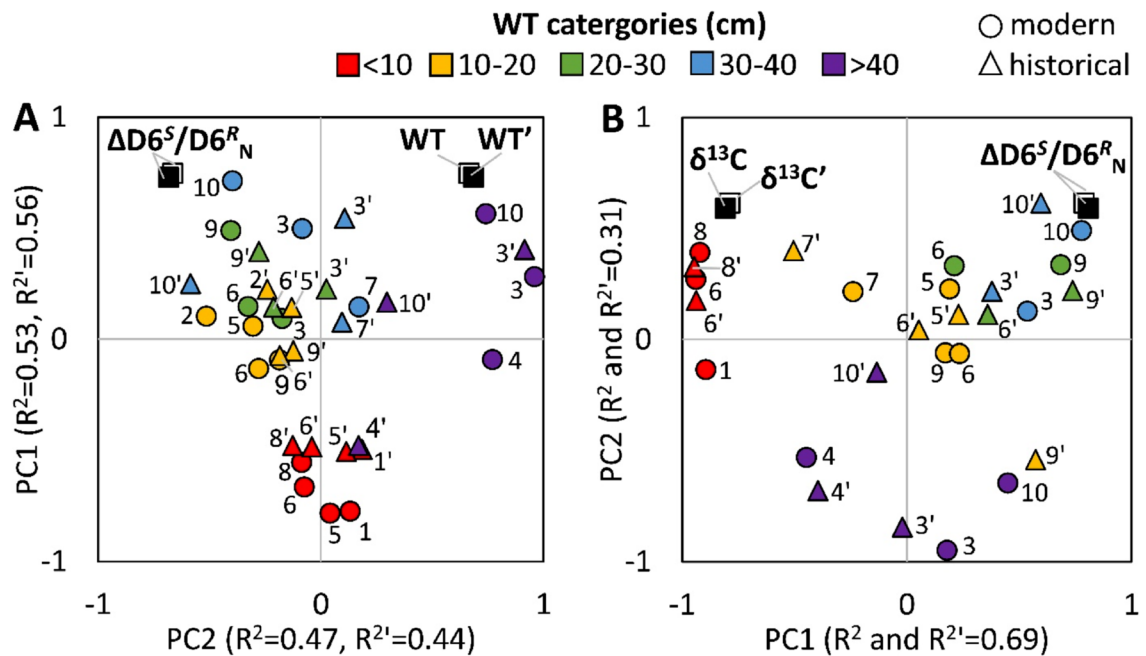


Figure 2. PCA biplots of the deuterium isotopomer ratio ($\Delta D6^S/D6^R_N$) of *Sphagnum* during the twentieth century and (A) the modern water table depth (WT, circles) and the historical water table depth inferred from testate amoebae data from literature (WT', triangles), and (B) modern *Sphagnum*- $\delta^{13}C$ ($\delta^{13}C$) and historical $\delta^{13}C$ data of ≥ 100 years-old *Sphagnum* samples ($\delta^{13}C'$). Colour coding indicates WT categories. Numbers indicate respective sites in Fig. 1A. Apostrophe indicates historical data point. Note that in (B) $\delta^{13}C$ data for site 2, site 3 (WT 20–30 cm) and site 5 (WT > 10 cm) are missing due to insufficient sample material.

and the modern WT depth, with historical WT depths from literature data (Fig. 2A). The results show that the general pattern remains the same for both modern and historical WT depths, indicating that the observed $\Delta D6^S/D6^R_N$ -response is not due to changes in WT during the twentieth century.

***Sphagnum* $\delta^{13}C$ as proxy for changes in water table depth.** The carbon isotopic signature ($\delta^{13}C$) of *Sphagnum* peat has been proposed as proxy for surface moisture^{27,36,45,46}. Therefore, we tested the use of $\delta^{13}C$ as a potential indicator of changes in WT depth by measuring the $\delta^{13}C$ of both modern and ≥ 100 years-old whole-*Sphagnum* tissues. Regression analysis revealed a highly significant correlation between $\delta^{13}C$ in modern *Sphagnum* and the present WT depth ($R^2=0.67$, $p<0.001$, Fig. S3A) confirming that $\delta^{13}C$ reflects changes in WT depth. The $\delta^{13}C$ values became more negative (*i.e.* more depleted) with increasing WT depth, from $-25.8 \pm 0.2\text{‰}$ (average \pm SE) at WT depths < 10 cm to $-30.3 \pm 0.5\text{‰}$ (average \pm SE) at WT depths > 60 cm below surface. For ≥ 100 years-old *Sphagnum*, $\delta^{13}C$ also correlated significantly with the historical WT depth inferred from testate amoebae data in Table 2 ($R^2=0.31$, $p<0.002$; Fig. S3B). Thus, both modern and historical *Sphagnum* showed the same trend (with slopes of 0.07 and 0.05, respectively), indicating that the WT depth ≥ 100 years ago was similar to that today. The PCA further confirmed that the pattern between the $\Delta D6^S/D6^R_N$ -response and modern *Sphagnum*- $\delta^{13}C$ values remained the same for the historical $\delta^{13}C$ values from ≥ 100 years-old *Sphagnum* samples (Fig. 2B). These results support that changes in WT during the twentieth century were generally small for the sites investigated, and not relevant to the isotopomer response.

Discussion

Our results show that the increase in atmospheric CO_2 during the twentieth century suppressed photorespiration relative to C assimilation in *Sphagnum* mosses, thus increasing the potential net photosynthesis. However, this suppression is strongly dependent on the moisture status of the moss. High moisture contents, typical for *Sphagnum* grown at WT depths < 10 cm, resulted in no significant suppression of photorespiration, with a mean $\Delta D6^S/D6^R_N$ value of 0.010 ($p>0.05$; Figs. 1, and S1). In contrast, the mean $\Delta D6^S/D6^R_N$ for WT depths between 10 and 40 cm was 0.066 ($p<0.05$), clearly reflecting a strong suppression of photorespiration. This latter response is identical to that obtained from CO_2 manipulation experiments with higher C_3 plants and corresponds to an increase in net photosynthesis of 35%, assuming constant ribulose 1,5-bisphosphate (RuBP) turnover rates^{26,47}. The similarity of the kinetic properties of Rubisco between different C_3 plants (including mosses)⁴⁸, suggests that the observed response in *Sphagnum* also corresponds to an increase in net photosynthesis of 35%. Conversely, the low $\Delta D6^S/D6^R_N$ value for *Sphagnum* grown at WT < 10 cm indicates no significant increase in net photosynthesis. This suggests that hollow and lawn *Sphagnum* communities that experience high WT do not profit from CO_2 fertilization. However, CO_2 fertilization is beneficial in mire structures that experience intermediate WT

depths, mostly hummocks, and may therefore stimulate hummock formation and topographic development as atmospheric CO₂ concentrations rise.

Some factors may limit the CO₂ fertilization effect in hummocks. In particular, our data show that a very low WT (> 40 cm) has a negative effect on CO₂ fertilization, *i.e.* on the suppression of photorespiration: the mean $\Delta D6^S/D6^R_N$ value for samples in the > 40 cm WT group was 0.016 ($p > 0.05$; Figs. 1, and S1). This indicates that *Sphagnum* mosses do not respond to increased atmospheric CO₂ under water limiting conditions, *i.e.* drought. Climate modelling of peatland C fluxes indicates that *Sphagnum* gross primary production decreases significantly at WT > 40 cm⁴⁹. Concomitantly, increased releases of CO₂ from sub-surface peat decomposition during drought^{50,51} may decouple the mosses' response to changes in atmospheric CO₂.

The D6^S/D6^R ratio of *S. fuscum* responded strongly to experimental manipulation of the CO₂ concentration²⁷, rising by 0.03 on average ($\Delta D6^S/D6^R_N$) when CO₂ levels increased by 120 ppm at a WT of 20 cm. In *S. fuscum* samples from peat cores with WT depths > 10 cm, the suppression of photorespiration ($\Delta D6^S/D6^R_N$) was 0.06 on average in response to a CO₂ concentration increase of ca. 100 ppm (Fig. 1). This suggests that the response to changes in atmospheric CO₂ levels under field conditions has been stronger than in growth chambers. In the field, environmental conditions such as light and nutrient levels may differ from the growth chamber conditions^{52,53}. Whether these factors affect the CO₂-driven suppression of photorespiration requires further investigation.

The peat core data in this study showed that higher CO₂ concentrations did not cause any suppression of photorespiration in *S. majus* grown at typical WT depths close to the mire surface ($\Delta D6^S/D6^R_N$: 0.00, Fig. 1). This result is consistent with the response observed in CO₂ manipulation experiments with *S. majus* for WT levels of 0 and 7 cm ($\Delta D6^S/D6^R_N$: 0.00)²⁷. Overall, the growth chamber experiments showed that water-saturating conditions prevent the suppression of photorespiration in both hummock and lawn *Sphagnum* species. The responses of the D6^S/D6^R ratio and $\delta^{13}C$ in our global dataset (Figs. 1, 2, S1, S2) are consistent with these results and demonstrate that a WT depth deeper than 10 cm is needed to maximize photosynthetic C fluxes in *Sphagnum*. Under these conditions, the mosses have the strongest potential to respond to the CO₂ fertilization effect.

The ANOVA (Table 1) showed a significant effect of the subgenus on the D6^S/D6^R ratio. Species of the section SPHAGNUM had generally lower D6^S/D6^R ratios than ACUTIFOLIA species, suggesting that the relative rate of photorespiration is lower in SPHAGNUM species. The ratio of photorespiration to photosynthesis is directly related to the intracellular CO₂ concentration (c_i) at the site of Rubisco carboxylation⁵⁴, suggesting differences in c_i between these two subgenera. Distinct leaf anatomical traits are responsible for different water holding capacities of these two subgenera⁵⁵, and potentially influence c_i . Altogether, this indicates that species of the subgenus SPHAGNUM have higher photosynthetic capacities than ACUTIFOLIA species, assuming that the RuBP turnover rates are similar.

Concerning the CO₂-driven suppression of photorespiration, both ACUTIFOLIA and SPHAGNUM species showed a high suppression of photorespiration, and no difference in this response between these two subgenera (average $\Delta D6^S/D6^R_N = 0.05$ for both). Thus, no significant interaction was found between CO₂ and subgenus (Table 1). In contrast, species of the subgenus CUSPIDATA showed no suppression of photorespiration (Fig. 1). Unlike the ACUTIFOLIA and SPHAGNUM samples (WT range 8 to 67 cm, both), the CUSPIDATA samples came from high WT cores (WT ca. 5 cm), making it impossible to determine whether this response is species-specific. However, CUSPIDATA species require high WT levels to maintain growth⁵⁶, suggesting that they will not respond to changes in atmospheric CO₂ in any case.

Our dataset revealed that the extent of the CO₂-driven suppression of photorespiration in *Sphagnum* mosses depends on the WT depth at the time of moss photosynthesis. To exclude potential effects of changes in WT during the twentieth century on the suppression of photorespiration, we estimated historical changes in WT by both measured *Sphagnum*- $\delta^{13}C$ data and published testate amoebae data (Table 2; Fig. 2). Both datasets revealed no relationship between the observed suppression of photorespiration and historical changes in WT. These results support our assumption that changes in hydrological conditions during the twentieth century did not attenuate the suppression of photorespiration caused by rising atmospheric CO₂ levels.

Moreover, we tested potential effects of changes in temperature and precipitation during the twentieth century on the CO₂-driven suppression of photorespiration ($\Delta D6^S/D6^R_N$). Our data did not indicate any relationship between the changes in temperature or precipitation during the twentieth century and the suppression of photorespiration (Table 2), supporting that these changes do not attenuate the observed response. The absence of an effect of temperature on the suppression of photorespiration is consistent with results from climate chamber experiments²⁷, where a temperature increase of 5 °C did not affect the magnitude of suppressed photorespiration. However, the photorespiration to photosynthesis (D6^S/D6^R) ratio increased slightly with elevated temperature (0.002 °C⁻¹)²⁷. Thus, the concomitant increase in temperature with atmospheric CO₂ during the twentieth century may have reduced the CO₂-driven suppression of photorespiration by approximately 0.002 units (for a temperature increase of 1 °C)⁸.

On the molecular scale, the D6^S/D6^R ratio reflects changes in the Rubisco oxygenation to carboxylation flux ratio. Here we extended this molecular model to study global responses in these metabolic C fluxes to environmental drivers in *Sphagnum*. Our results indicate that ongoing increases in atmospheric CO₂ suppress photorespiration relative to C assimilation in *Sphagnum*. According to photosynthesis models, this suppression may increase C uptake by up to 35% (depending on the WT level), which points towards an increase in net primary production (NPP) during the twentieth century. However, NPP is influenced by many other factors such as temperature, precipitation and sink limitations^{9,57}. Modelling of peatland C dynamics^{49,58} suggests that temperature and precipitation have opposing influences on the C uptake response to the recent increase in atmospheric CO₂. An increase in temperature combined with a decrease in precipitation reduces C uptake, whereas a small increase in temperature combined with a large increase in precipitation results in enhanced C uptake. We found a significant interaction between the mean annual/summer temperature and WT during the twentieth century, indicating a possible link between the observed changes in metabolic fluxes on the molecular level and

global peat C assimilation. Thus, upscaling of the isotopomer data to global responses in peat C fluxes provide valuable information for the mechanistic understanding of photosynthetic responses of *Sphagnum* mosses to ongoing and future climate changes.

Conclusion

Here we used deuterium isotopomers to study global responses in photosynthetic C fluxes in *Sphagnum* mosses to the twentieth century's increase in atmospheric CO₂. This method allowed us to upscale changes in metabolic C flux ratios from the molecular level to the global scale. We were able to track historical changes of metabolic C fluxes over long time scales using peat archives and link these results to observations from short-term manipulation experiments. Thus, our results will help to: (i) develop mechanistic models of global metabolic C fluxes, (ii) assess the role of peatlands for the global C budget during the twentieth century, and (iii) improve the prediction of future responses of peatlands to increases in atmospheric CO₂ and climate change. Furthermore, our results point out that mire structures with intermediate WT depths, such as hummocks, will benefit strongly from CO₂ fertilization, unlike lawn and hollow *Sphagnum* communities that often experience high WT depths.

Materials and methods

Plant material-peat cores. Hummock and lawn peat cores were retrieved from 10 sites located in Sweden (2), Italy (2), Canada (3), China (1), Argentina (1), and Australia (1) between 2014 and 2018. The sites' latitudes ranged from 55°S to 64°N, their mean annual air temperatures from −3.9 to 6.3 °C, mean annual precipitation levels from 369 to 1270 mm, and elevations from 35 to 1700 m asl. Detailed descriptions of each site are provided in the supplement (Table S3). Historical *Sphagnum* samples were retrieved from peat depths between 30 and 40 cm, except in the cores from southern Argentina (60 cm). All historical samples were found to be approximately 100 years or older, based on ²¹⁰Pb radiometric dating or estimates obtained using published age-depth profiles for each site (Table S1). The atmospheric CO₂ concentration when the historical *Sphagnum* samples formed was estimated for the respective year and ranged between 280 and 310 ppm (Table S1)⁵⁹. Since no major changes in atmospheric CO₂ levels occurred between year 0 and 1900, uncertainties in the age-estimates are not expected to have major effects on the estimated CO₂ concentration.

Peat cores were extracted using a sharp knife or a peat corer, yielding cores with dimensions of 8 × 8 cm or diameters of 10 cm, respectively. Peat cores were either wrapped in plastic film and stored at −20 °C or sliced into 2 cm sections, oven dried (at 60 °C), and transferred to Ziploc-bags before further transport to Sweden. In the case of frozen cores, the topmost and bottom-most 2 cm were sliced off and thawed, and vascular plant material and mosses other than *Sphagnum* were removed. In cases where no intact species could be retrieved from the bottom of the core (six cores), the material was washed through a series of sieves (mesh sizes: 3 mm, 1.6 mm, 0.8 mm and 0.5 mm). The residue of the 0.5 mm sieve consisted almost exclusively of *Sphagnum* leaves. *Sphagnum* species from the top and bottom of the core were identified using a stereomicroscope and a binocular microscope (100 and 400×). The species were identified according to literature^{60–63}. Peat cores in which the dominant *Sphagnum* species/subgenus differed between top and bottom were excluded because such differences indicate a change in microtopography. After processing as described above, samples were dried at 60 °C for 3 days. The WT depth in Table S1 was measured at the time of sampling, which happened generally during the summer months. In order to consider local WT fluctuations, we compared the WT measurements with mean seasonal and testate amoebae inferred WT data from the literature for each site respectively (Table S4). A PCA biplot confirmed that the WT measurements match well with mean growing season WT depths reported in the literature (Fig. S4).

Sample preparation for deuterium isotopomer measurements. The dried *Sphagnum* samples were ground to a fine powder at 30 Hz for 2 min using a MM 400 ball mill (Retsch, Haan, Germany), and 200–700 mg portions were used to prepare samples for Deuterium isotopomer measurements. Glucose-containing structural polymers were hydrolyzed to glucose and converted to 1,2-O-isopropylidene- α -D-glucopyranose according to established protocols⁶⁴. To remove contamination by a mannose derivative whose NMR signals overlap with those of the glucose derivative, an oxidation step was applied as previously described²⁷. The derivative was subsequently converted into 3,6-anhydro-1,2-O-isopropylidene- α -D-glucopyranose following published procedures⁶⁵. The latter compound was purified by flash chromatography using silica gel and diethyl ether. Pure fractions were identified by thin-layer-chromatography and pooled. Diethyl ether was evaporated, the sample was washed with amylene-stabilized chloroform, and its purity was checked by ¹H-NMR.

Deuterium isotopomer quantification. For NMR measurements of intramolecular deuterium abundances, each sample of the glucose derivative prepared as described above was dissolved in a mixture of 83% v/v acetonitrile, 17% C₆F₆, and 0.01% C₆D₆, then transferred to a 5-mm NMR tube with a PTFE valve (J. Young Scientific Glassware Ltd., Windsor, U.K.) containing ca. 5 mg of NaHCO₃. Deuterium NMR spectra were acquired and processed as previously described⁶⁴, using an AVANCE III 850 spectrometer (Bruker BioSpin GmbH, Rheinstetten, Germany) equipped with a ¹⁹F lock and a cryogenic probe optimized for deuterium detection. Deuterium NMR spectra were integrated by deconvolution with a Lorentzian line shape fit, using TopSpin™ 3.2 (Bruker BioSpin GmbH, Rheinstetten, Germany). The D₆^S/D₆^R isotopomer ratio was determined as the ratio of the integrals of the D₆^S and D₆^R signals²⁶. For each sample, five to eight spectra were recorded and the average D₆^S/D₆^R ratio was calculated.

C-isotope analysis. C-isotopic signatures ($\delta^{13}\text{C}$) of dry moss tissue samples (ca. 5 mg) were analyzed by conversion into CO₂ by combustion and quantification by mass spectrometry⁶⁶, using an elemental analyser (Flash EA 2000, Thermo Fisher Scientific, Bremen, Germany) coupled to an isotope ratio mass spectrometer

(DeltaV, Thermo Fisher Scientific, Bremen, Germany). The data were corrected for drift and non-linear sample size effects. For quantification, we used laboratory standards consisting of wheat and maize flours calibrated against two certified $\delta^{13}\text{C}$ reference standards: IAEA-CH-6, and USGS40.

Statistical analysis. Prior to statistical analysis, the samples from the top and bottom of each core were assigned as high and low CO_2 respectively. Based on their present WT depths, samples were divided into five different groups: < 10, 10–20, 21–30, 31–40 and > 40 cm below surface. Individual *Sphagnum* species were grouped into their subgenera: ACUTIFOLIA (*S. fuscum*, *S. warnstorfi* & *S. capillifolium*), SPHAGNUM (*S. magellanicum*, *S. divinium/medium*, *S. papillosum* & *S. cristatum*), and CUSPIDATA (*S. cuspidatum* & *S. majus*; Table S1). Geographical locations were assigned according to Table S3. Effects of these different variables on the $\text{D}_6^{\text{S}}/\text{D}_6^{\text{R}}$ ratio were assessed by ANOVA, which was done in R (version 3.6.1, RStudio, Inc.) by computing linear mixed effect models using the *lmer()* function of the *lme4* package⁶⁷. To perform ANOVA on the random effect and the fixed effects, the functions *ranova()* and *anova()* were applied respectively. Post-hoc Fisher's LSD tests with Benjamini–Hochberg correction were computed (in Fig. S1), using the *LSD.test()* function, to account for false discovery rates⁶⁸. To test for multicollinearity among the variables, we calculated the variance inflation factors (VIF) using the *vif()* function of the *car* package. All variables/factors and interaction terms showed a VIF of less than five (range 2.7–4.3), indicating no significant collinearity⁶⁹. Effect of changes in WT, temperature and precipitation were tested by ANOVA, by computing linear models using the *lm()* function and automated stepwise model selection based on Akaike's information criterion using the *step()* function of the *stats* package⁷⁰. PCA was performed by using the SIMCA-P software package version 16 (Umetrics, Umeå, Sweden). Biplots were created by using the *biplot* function, which displays both PCA scores, and the correlation scaled loadings of principle component 1 and 2. All other statistical analyses were performed in Excel. Student's t-tests were one-tailed assuming unequal variance.

Climate data analysis. Climate data such as annual temperature and precipitation as well as summer temperature and precipitation (June–August and December–February for northern and southern hemisphere, respectively) were obtained from existing climate reconstruction data^{33–35}. Changes during the twentieth century were estimated by calculating the 3-year averages around the approximate ages (± 1 year) estimated for the modern and historical samples (Table S5). Luterbacher et al.³³ and Pauling et al.³⁴ provide a dataset of seasonal (3-month) mean air temperatures and total precipitation levels respectively, for Europe (defined as the region between 35.25°N and 69.75°N, and 24.75°W and 39.75°E), covering the period from 1500 to 2002 with a 0.5° gridded resolution (<https://crudata.uea.ac.uk/cru/projects/soap/data/>). Willmott and Matsuura³⁵ provide a global dataset of mean monthly air temperatures and total precipitation from 1900 to 2017 with a 0.5° gridded resolution (<http://climate.geog.udel.edu/~climate>). Consequently, the Willmott and Matsuura dataset³⁵ was used to estimate the climate after 1900 and the Luterbacher et al. and Pauling et al. dataset^{33,34} to estimate the climate before 1900. The two databases showed differences specifically for the Italian sites; therefore, data for 1860 and 1880 were normalized against the more recent data (1990–2000) of Willmott and Matsuura³⁵. Australian precipitation data from before 1900 were obtained from the Bureau of Meteorology, Australian Government, 2020 (<http://www.bom.gov.au/climate/data>). Temperature data were not available for the Australian site and were therefore estimated for 1900 using the Willmott and Matsuura dataset³⁵. The southern Argentinian samples were estimated to be ≈ 860 years old, thus the temperature and precipitation data for the Argentinian site were estimated according to other climate models^{71,72}.

Received: 26 July 2021; Accepted: 12 November 2021

Published online: 31 December 2021

References

- Frolking, S. et al. Peatlands in the earth's 21st century climate system. *Environ. Rev.* **19**, 371–396 (2011).
- Loisel, J. et al. A database and synthesis of northern peatland soil properties and Holocene carbon and nitrogen accumulation. *Holocene* **24**(9), 1028–1042 (2014).
- Belyea, L. R. & Malmer, N. Carbon sequestration in peatland: Patterns and mechanisms of response to climate change. *Glob. Change Biol.* **10**(7), 1043–1052 (2004).
- Gallego-Sala, A. V. et al. Latitudinal limits to the predicted increase of the peatland carbon sink with warming. *Nat. Clim. Change* **8**(10), 907–913 (2018).
- Harden, J. W., Sundquist, E. T., Stallard, R. F. & Mark, R. K. Dynamics of soil carbon during deglaciation of the Laurentide ice-sheet. *Science* **258**(5090), 1921–1924 (1992).
- Gorham, E., Lehman, C., Dyke, A., Janssens, J. & Dyke, L. Temporal and spatial aspects of peatland initiation following deglaciation in North America. *Quat. Sci. Rev.* **26**(3–4), 300–311 (2007).
- Indermühle, A. et al. Holocene carbon-cycle dynamics based on CO_2 trapped in ice at Taylor Dome, Antarctica. *Nature* **398**(6723), 121–126 (1999).
- IPCC. In *Climate Change (2013): The Physical Science Basis. Contribution of Working Group I to the Fifth Assessment Report of the Intergovernmental Panel on Climate Change* (eds Stocker T.F. et al.) (Cambridge University Press, 2013).
- Charman, D. J. et al. Climate-related changes in peatland carbon accumulation during the last millennium. *Biogeosciences* **10**(2), 929–944 (2013).
- Loisel, J. & Yu, Z. Recent acceleration of carbon accumulation in a boreal peatland, south central Alaska. *J. Geophys. Res. Biogeosci.* **118**, 41–53 (2013).
- Lund, M. et al. Variability in exchange of CO_2 across 12 northern peatland and tundra sites. *Glob. Change Biol.* <https://doi.org/10.1111/j.1365-2486.2009.02104.x> (2010).

12. Yang, G. *et al.* Responses of CO₂ emission and pore water DOC concentration to soil warming and water table drawdown in Zoige Peatlands. *Atmos. Environ.* **152**, 323–329 (2017).
13. Laine, A. M. *et al.* Warming impacts on boreal fen CO₂ exchange under wet and dry conditions. *Glob. Change Biol.* **25**(6), 1995–2008 (2019).
14. Pancotto, V., Holl, D., Escobar, J., Castagnani, M. F. & Kutzbach, L. Cushion bog plant community responses to passive warming in southern Patagonia. *Biogeosciences* **18**(16), 4817–4839 (2020).
15. Gunnarsson, U. Global patterns of *Sphagnum* productivity. *J. Bryol.* **27**, 269–279 (2005).
16. Limpens, J. & Berendse, F. How litter quality affects mass loss and N loss from decomposing *Sphagnum*. *Oikos* **103**(3), 537–547 (2003).
17. Hajek, T., Ballance, S., Limpens, J., Zijlstra, M. & Verhoeven, J. T. A. Cell-wall polysaccharides play an important role in decay resistance of *Sphagnum* and actively depressed decomposition in vitro. *Biogeochemistry* **103**, 45–57 (2011).
18. Dorrepaal, E. *et al.* Carbon respiration from subsurface peat accelerated by climate warming in the subarctic. *Nature* **460**, 616–619. <https://doi.org/10.1038/nature08216> (2009).
19. Loisel, J. *et al.* Expert assessment of future vulnerability of the global peatland carbon sink. *Nat. Clim. Change* **11**, 70–77 (2021).
20. Van der Heijden, E., Verbeek, S. K. & Kuiper, P. J. C. Elevated atmospheric CO₂ and increased nitrogen deposition: Effects on C and N metabolism and growth of the peat moss *Sphagnum recurvum* P. Beauv. Var. mucronatum (Russ.) Warnst. *Glob. Change Biol.* **6**(2), 201–212 (2000).
21. Berendse, F. *et al.* Raised atmospheric CO₂ levels and increased N deposition cause shifts in plant species composition and production in *Sphagnum* bogs. *Glob. Change Biol.* **7**(5), 591–598 (2001).
22. Heijmans, M. M. P. D. *et al.* Effects of elevated carbon dioxide and increased nitrogen deposition on bog vegetation in the Netherlands. *J. Ecol.* **89**(2), 268–279 (2001).
23. Heijmans, M. M. P. D., Klees, H., de Visser, W. & Berendse, F. Response of a *Sphagnum* bog plant community to elevated CO₂ and N supply. *Plant Ecol.* **162**(1), 123–134 (2002).
24. Mitchell, E. A. D. *et al.* Contrasted effects of increased N and CO₂ supply on two keystone species in peatland restoration and implications for global change. *J. Ecol.* **90**(3), 529–533 (2002).
25. Toet, S. *et al.* Moss responses to elevated CO₂ and variation in hydrology in a temperate lowland peatland. *Plant Ecol.* **182**(1–2), 27–40 (2006).
26. Ehlers, I. *et al.* Detecting long-term metabolic shifts using isotopomers: CO₂-driven suppression of photorespiration in C₃ plants over the 20th century. *Proc. Natl. Acad. Sci. USA* **112**(51), 15585–15590 (2015).
27. Serk, H., Nilsson, M. B., Figueira, J., Wieloch, T. & Schleucher, J. CO₂ fertilization of *Sphagnum* peat mosses is modulated by water table level and other environmental factors. *Plant Cell Environ.* <https://doi.org/10.1111/pce.14043> (2021).
28. Walker, A. P. *et al.* Integrating the evidence for a terrestrial carbon sink caused by increasing atmospheric CO₂. *New Phytol.* <https://doi.org/10.1111/nph.16866> (2020).
29. Schipperges, B. & Rydin, H. Response of photosynthesis of *Sphagnum* species from contrasting microhabitats to tissue water content and repeated desiccation. *New Phytol.* **140**(4), 677–684 (1998).
30. Robroek, B. J. M., Schouten, M. G. C., Limpens, J., Berendse, F. & Poorter, H. Interactive effects of water table and precipitation on net CO₂ assimilation of three co-occurring *Sphagnum* mosses differing in distribution above the water table. *Glob. Change Biol.* **15**, 680–691 (2009).
31. Weston, D. J. *et al.* *Sphagnum* physiology in the context of changing climate: Emergent influences of genomics, modelling and host–microbiome interactions on understanding ecosystem function. *Plant Cell Environ.* **38**(9), 1737–1751 (2015).
32. Bengtsson, F., Granath, G. & Rydin, H. Photosynthesis, growth, and decay traits in *Sphagnum*—A multispecies comparison. *Ecol. Evol.* **6**(19), 3325–3341 (2016).
33. Luterbacher, J., Dietrich, D., Xoplaki, E., Grosjean, M. & Wanner, H. European seasonal and annual temperature variability, trends, and extremes since 1500. *Science* **303**, 1499–1503 (2004).
34. Pauling, A., Luterbacher, J., Casty, C. & Wanner, H. Five hundred years of gridded high-resolution precipitation reconstructions over Europe and the connection to large-scale circulation. *Clim. Dyn.* **26**, 387–405 (2006).
35. Willmot, C. J., & Matsuura, K. Terrestrial air temperature and precipitation: Gridded monthly time series (1900–2017), (V 5.01 added 6/1/18). http://climate.geog.udel.edu/~climate/html_pages/Global2017/README.GlobalTst2017.html and README.GlobalTSP2017.html (2018).
36. Loisel, J., Garneau, M. & Hélie, J.-F. *Sphagnum* δ¹³C values as indicators of palaeohydrological changes in a peat bog. *Holocene* **20**(2), 285–291 (2010).
37. Swindles, G. T. *et al.* Widespread drying of European peatlands in recent centuries. *Nat. Geosci.* **12**, 922–928 (2019).
38. Pelletier, N. *et al.* Influence of Holocene permafrost aggradation and thaw on the paleoecology and carbon storage of a peatland complex in northwestern Canada. *Holocene* **27**(9), 1391–1405 (2017).
39. Talbot, J., Richard, P. J. H., Roulet, N. T. & Booth, R. K. Assessing long-term hydrological and ecological responses to drainage in a raised bog using paleoecology and a hydrosequence. *J. Veg. Sci.* **21**, 143–156 (2010).
40. Kopp, B. J. *et al.* Impact of long-term drainage on summer groundwater flow patterns in the Mer Bleue peatland, Ontario, Canada. *Hydrol. Earth Sci.* **17**, 3485–3498 (2013).
41. Van Bellen, S. *et al.* Late-Holocene climate dynamics recorded in the peat bogs of Tierra del Fuego, South America. *Holocene* **26**(3), 489–501 (2016).
42. De Jong, R., Schoning, K. & Björck, S. Increased aeolian activity during humidity shifts as recorded in a raised bog in south-west Sweden during the past 1700 years. *Clim. Past* **3**, 411–422 (2007).
43. Kunshan, B. *et al.* A 100-year history of water level change and driving mechanism in Heilongjiang River basin wetlands. *Quat. Sci.* **38**(4), 981–995 (2018).
44. Zheng, X. The reconstruction of moisture availability in south-eastern Australia during the Holocene. PhD thesis, University of New South Wales, Sydney (2018).
45. Loader, N. J. *et al.* Measurements of hydrogen, oxygen and carbon isotope variability in *Sphagnum* moss along a micro-topographical gradient in a southern Patagonian peatland. *J. Quat. Sci.* **31**(4), 426–435 (2016).
46. Xia, Z. *et al.* Environmental controls on the carbon and water (H and O) isotopes in peatland *Sphagnum* mosses. *Geochim. Cosmochim. Acta* **277**, 265–284 (2020).
47. Sharkey, T. D. Estimating the rate of photorespiration in leaves. *Physiol. Plant.* **73**, 147–152 (1988).
48. Flamholz, A. I. *et al.* Revisiting trade-offs between Rubisco kinetic properties. *Biochemistry* **58**, 3365–3376 (2019).
49. Wu, J. H. & Roulet, N. T. Climate change reduces the capacity of northern peatlands to absorb the atmospheric carbon dioxide: The different responses of bogs and fens. *Glob. Biogeochem. Cycles* <https://doi.org/10.1002/2014GB004845> (2014).
50. Fenner, N. & Freeman, C. Drought-induced carbon loss in peatlands. *Nat. Geosci.* **4**, 895–900 (2011).
51. Lund, M., Christensen, T. R., Lindroth, A. & Schubert, P. Effects of drought conditions on the carbon dioxide dynamics in a temperate peatland. *Environ. Res. Lett.* **7**, 045704. <https://doi.org/10.1088/1748-9326/7/4/045704> (2012).
52. Chong, M., Humphreys, E. R. & Moore, T. R. Microclimatic response to increasing shrub cover and its effect on *Sphagnum* CO₂ exchange in a bog. *Ecoscience* **19**, 89–97 (2012).
53. Fritz, C. *et al.* Nutrient additions in pristine Patagonian *Sphagnum* bog vegetation: Can phosphorus addition alleviate (the effects of) increased nitrogen loads. *Plant Biol.* **14**, 491–499 (2012).

54. Farquhar, G. D., Ehleringer, J. R. & Hubick, K. T. Carbon isotope discrimination and photosynthesis. *Annu. Rev. Plant Physiol. Plant Mol. Biol.* **40**, 503–537 (1989).
55. Bengtsson, F., Granath, G., Cronberg, N. & Rydin, H. Mechanisms behind species-specific water economy responses to water level drawdown in peat mosses. *Ann. Bot.* **126**(2), 219–230 (2020).
56. Nijp, J. J. *et al.* Can frequent precipitation moderate the impact of drought on peatmoss carbon uptake in northern peatlands?. *New Phytol.* **203**(1), 70–80 (2014).
57. Limpens, J., Berendse, F. & Klees, H. How phosphorous availability affects the impact of nitrogen deposition on *Sphagnum* and vascular plants in bogs. *Ecosystems* **7**, 793–804 (2004).
58. Wu, J. H., Roulet, N. T., Nilsson, M., Lafleur, P. & Humphreys, E. Simulating the carbon cycling of Northern peat lands using a land surface scheme coupled to a Wetland Carbon Model (CLASS3W-MWM). *Atmos. Ocean* **50**(4), 487–506 (2012).
59. Etheridge D. M., Steele L. P., Langenfelds R. L., Francey R. J., Barnola J. M., & Morgan V. I. Historical CO₂ records from the law dome DE08, DE08-2, and DSS ice cores (1006 A.D.–1978 A.D). <https://doi.org/10.3334/CDIAC/ATG.011> (Carbon Dioxide Information Analysis Center (CDIAC); Oak Ridge National Laboratory (ORNL), 1998).
60. Laine, J. *et al.* The intrinsic beauty of *Sphagnum* Mosses—A Finnish guide to Identification. University of Helsinki. *Dept. For. Sci. Publ.* **2**, 1–191 (2011).
61. Grover, S. P. P., Baldock, J. A. & Jacobsen, G. E. Accumulation and attrition of peat soils in the Australian Alps: Isotopic dating evidence. *Austral. Ecol.* **37**, 510–517 (2012).
62. Kleinbecker, T., Hölzel, N. & Vogel, A. Gradients of continentality and moisture in south Patagonian ombrotrophic peatland vegetation. *Folia Geobotanica* **42**, 363–382 (2007).
63. Hassel, K. *et al.* *Sphagnum divinum* (sp. nov.) and *S. medium* Limpr. and their relationship to *S. magellanicum* Brid. *J. Bryol.* **40**, 197–222 (2018).
64. Betson, T. R., Augusti, A. & Schleucher, J. Quantification of deuterium isotopomers of tree-ring cellulose using nuclear magnetic resonance. *Anal. Chem.* **78**(24), 8406–8411 (2006).
65. Schleucher, J., Vanderveer, P., Markley, J. L. & Sharkey, T. D. Intramolecular deuterium distributions reveal disequilibrium of chloroplast phosphoglucose isomerase. *Plant Cell Environ.* **22**(5), 525–533 (1999).
66. Werner, R. A., Bruch, B. A. & Brand, W. A. ConFlo III—An interface for high precision $\delta^{13}\text{C}$ and $\delta^{15}\text{N}$ analysis with an extended dynamic range. *Rapid Commun. Mass Spectrom.* **13**(13), 1237–1241 (1999).
67. Bates, D., Mächler, M., Bolker, B. & Walker, S. Fitting linear mixed-effects models using lme4. *J. Stat. Softw.* **67**(1), 1–48 (2015).
68. Benjamini, Y. & Hochberg, Y. Controlling the false discovery rate: A practical and powerful approach to multiple testing. *J. R. Stat. Soc. B* **57**, 289–300 (1995).
69. Gareth, J., Witten, D., Hastie, T. & Tibshirani, R. *An Introduction to Statistical Learning: With Applications in R* (Springer Science+Business Media, 2013).
70. Venables, W. N. & Ripley, B. D. *Modern Applied Statistics with S* 4th edn. (Springer, 2002).
71. Lüning, S., Galka, M., Bamonte, F. P., Rodriguez, F. G. & Vahrenholt, F. The medieval climate anomaly in South America. *Quat. Int.* **508**, 70–87 (2019).
72. Schimpf, D. *et al.* The significance of chemical isotopic and detrital components in three coeval stalagmites from the superhumid southernmost Andes (53°S) as high-resolution paleo-climate proxies. *Quat. Sci. Rev.* **30**, 443–459 (2011).

Acknowledgements

The authors acknowledge the help provided by the ‘NMR for Life’ infrastructure supported by the Wallenberg and Kempe Foundations, and by SciLifeLab; the SLU Stable Isotope Laboratory (for C-isotope analysis) and financial support from the Swedish Research Council (Vetenskapsrådet), the Carl Tryggers Foundation and the Knut and Alice Wallenberg Foundation (#2015.0047). Australian peat samples were collected under Parks Victoria research permit No. 10008607. Argentinean peat samples were collected under SDSyA 078/13 and APN/28 research permit.

Author contributions

H.S., M.N., and J.S. planned and designed the research; M.N., S.G., K.K., J.L., T.M., J.T., W.M., V.P., X.W. and K.-H.K. sampled/provided the peat cores; C.O. and J.T. dated the peat cores; H.S. and I.E. prepared the peat samples for isotopomer analysis; E.B. identified the species composition of the peat samples; J.S. and H.S. acquired the NMR spectra; H.S. and T.W. analyzed the data; and H.S., M.N., and J.S. wrote the paper and all other co-authors contributed to revision of the paper.

Funding

Open access funding provided by Swedish University of Agricultural Sciences.

Competing interests

The authors declare no competing interests.

Additional information

Supplementary Information The online version contains supplementary material available at <https://doi.org/10.1038/s41598-021-02953-1>.

Correspondence and requests for materials should be addressed to M.B.N. or J.S.

Reprints and permissions information is available at www.nature.com/reprints.

Publisher’s note Springer Nature remains neutral with regard to jurisdictional claims in published maps and institutional affiliations.



Open Access This article is licensed under a Creative Commons Attribution 4.0 International License, which permits use, sharing, adaptation, distribution and reproduction in any medium or format, as long as you give appropriate credit to the original author(s) and the source, provide a link to the Creative Commons licence, and indicate if changes were made. The images or other third party material in this article are included in the article's Creative Commons licence, unless indicated otherwise in a credit line to the material. If material is not included in the article's Creative Commons licence and your intended use is not permitted by statutory regulation or exceeds the permitted use, you will need to obtain permission directly from the copyright holder. To view a copy of this licence, visit <http://creativecommons.org/licenses/by/4.0/>.

© The Author(s) 2021